Microporous and Mesoporous Materials 118 (2009) 427–434

Contents lists available at ScienceDirect

Microporous and Mesoporous Materials

journal homepage: www.elsevier.com/locate/micromeso

Porous layered oxide/Nafion® nanocomposite membranes for direct methanol fuel cell applications

Yeny Hudiono [a], Sunho Choi [b], Shu Shu [a], William J. Koros [a], Michael Tsapatsis [b], Sankar Nair [a,*]

[a] School of Chemical & Biomolecular Engineering, Georgia Institute of Technology, Atlanta, GA 30332-0100, USA
[b] Department of Chemical Engineering and Materials Science, University of Minnesota, Minneapolis, MN 55455, USA

ARTICLE INFO

Article history:
Received 12 August 2008
Received in revised form 14 September 2008
Accepted 15 September 2008
Available online 23 September 2008

Keywords:
Direct methanol fuel cell (DMFC)
Polyelectrolyte exchange membrane (PEM)
Porous materials
Layered silicates
Layered aluminophosphates

ABSTRACT

Nanocomposite membranes were prepared by exfoliating, intercalating and/or dispersing nanoporous layered aluminophosphate or silicate materials in Nafion®. Specifically, the layered aluminophosphate-triethylamine (APO-TE), aluminophosphate-isopropanolamine (APO-IPA), aluminophosphate-imidazole (APO-ImH), and the swollen layered silicate AMH-3, were used as selectively permeable barriers that can potentially block methanol permeation but maintain proton conductivity in the membrane. The presence of the layered materials in Nafion® membranes reduced the methanol permeability by up to an order of magnitude while maintaining proton conductivities close to that of neat Nafion® at room temperature. Small-angle X-ray scattering (SAXS) characterization shows substantial differences in microstructure of the nanocomposite membranes from that of neat Nafion®. The performance of the nanocomposite membranes was also found to be strongly dependent on the membrane pre-treatment conditions. Detailed comparison of our data to the previous literature indicates that for certain conditions of membrane preparation, the proposed approach yields promising results in controlling methanol and proton transport through membranes for direct methanol fuel cell (DMFC) applications.

1. Introduction

Significant rises in fossil fuel costs and global environmental concerns continue to increase the demand for new energy sources as well as better methods of energy utilization. Fuel cells are considered one of the viable alternatives for energy utilization, notably to generate power for automotive and portable electronics applications. A number of different types of fuel cells have been developed [1]. One of the most widely investigated types of fuel cells is the proton exchange membrane fuel cell (PEMFC), also known as a polyelectrolyte membrane fuel cell. It utilizes a polymeric electrolyte membrane (PEM), e.g. made of Nafion®, to conduct protons between the anode and the cathode. The protons are generated by the catalytic oxidation of the fuel at the anode. In hydrogen-based PEMFCs, molecular hydrogen (H_2) is used as the fuel. The generation and compression/storage of hydrogen for such fuel cells is a subject of extensive ongoing research [2]. On the other hand, alcohols such as methanol and ethanol (which can be manufactured from natural gas or biomass) can also be used as fuels. In this case, an alcohol/water mixture is catalytically oxidized at the anode to generate protons for conduction through the PEM. In particular, the direct methanol fuel cell (DMFC) utilizes methanol as the fuel, and is attractive for several reasons. It can operate in a wide temperature range (up to 150 °C); and it uses a liquid or vapor fuel that is easy to generate and store, and which has a much higher energy density (per unit volume) than compressed hydrogen. The DMFC is suitable for portable/mobile devices such as cell phones and laptops because it can deliver about 10 times the power density of a lithium battery [3] and does not require recharging (only a methanol fuel cartridge replacement). A number of companies have developed prototypes of cellular phones, laptops, and portable cameras powered by DMFCs [4]. It is envisaged that the worldwide market for DMFC technology will reach $2.6 bn by 2012 [5].

Although much progress has been made in DMFC technology, there are significant challenges to be overcome. The energy conversion efficiency of DMFCs is still low; only 32–40% of the chemical energy is converted to electrical energy. This is primarily due to two reasons: (i) the high rate of methanol loss by permeation (crossover) through the PEM and (ii) the low methanol oxidation rate at the anode. This paper is concerned with membranes that reduce methanol crossover. In addition to causing fuel wastage, the unoxidized methanol (that reaches the cathode by crossover from the anode) also affects the activity of the cathode catalyst for the reduction of oxygen to water. Ultimately, high methanol crossover decreases the overall efficiency and lifetime. Hence, low concentrations of methanol (<10 vol%) are used, whereas it is desirable to use much higher concentrations at the anode to reduce the volume of fuel required with no concurrent loss of efficiency. Recent work has also suggested that fuel crossover may be one of the necessary fac-

* Corresponding author.
E-mail address: sankar.nair@chbe.gatech.edu (S. Nair).

1387-1811/$ - see front matter © 2008 Elsevier Inc. All rights reserved.
doi:10.1016/j.micromeso.2008.09.017

tors for the creation of reactive free radicals at the cathode, which attack the polymeric membrane material and may lead to catastrophic failure of the PEM [6–9]. Due to the above reasons, the pursuit of new membrane materials that significantly reduce fuel crossover while maintaining high proton conductivity has been of considerable interest. For example, the report of the DOE BES Workshop on Hydrogen Production, Storage, and Use identified "improving gas impermeability while retaining high proton conductivity of membranes for PEMFCs" as a high-priority research direction [10]. The most widely used and commercialized PEM material is Nafion®, manufactured by DuPont. Nafion® is an ionic polymer that comprises a polyfluorocarbon backbone with a high concentration of pendant sulfonic acid groups that facilitate proton transport. Unfortunately, Nafion® exhibits high methanol crossover. Several initial attempts to reduce the methanol crossover were implemented by increasing the membrane thickness, or decreasing methanol concentration [5]. Nevertheless, only a moderate improvement in performance was attained. A number of more recent approaches have been reviewed by several authors [11–13] and will be discussed in some detail below.

In this paper, we first review concisely the state-of-the-art in the development of improved PEM materials for DMFCs. We highlight both the differences in approach taken by various groups, as well as some important differences in experimental methods that should be considered when comparing results of different approaches. We compile a diagram that represents the state-of-the-art in engineering the methanol permeability and proton conductivity in PEMs. We then report results concerning a novel concept for controlling the methanol crossover and proton conductivity of PEM materials, based upon the fabrication of polymer/inorganic nanocomposites containing porous layered oxide materials (Fig. 1). We propose that porous layered silicate or aluminophosphate materials [14–17] exfoliated/intercalated/dispersed in Nafion® or other ionomers can act as selectively permeable barriers that block methanol permeation but do not reduce (or may potentially even increase) the proton conductivity. These dual properties

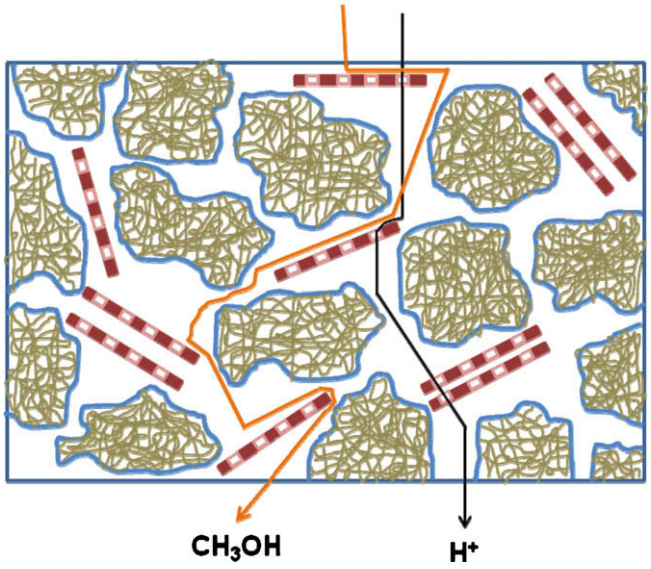

Fig. 1. Schematic of Nafion®/nanoporous oxide layered composite membrane. It shows the intercalated or exfoliated oxide layered materials embedded/dispersed in the hydrophilic (water-containing) sections of the Nafion® two-phase structure. This schematic is not intended as an accurate description of the microstructure of such membranes but only as a qualitative aid to visualization. The green areas represent the hydrophobic sections of Nafion®, the blue borders represent the sulfonic acid groups, and the red layers represent the porous layered materials. (For interpretation of the references to colour in this figure legend, the reader is referred to the web version of this article.)

can be obtained because of the combination of small pore size of a few angstroms (which can permeate protons selectively over methanol) as well as a high aspect ratio (which creates highly tortuous paths for diffusing methanol molecules). In this first study, we fabricated and characterized several types of Nafion®-based nanocomposite membranes, containing 5 wt% of different porous layered materials such as the aluminophosphates $3[CH_3CH_2NH_3][Al_3P_4O_{16}]$ (APO-TE) [14], $[NH_3CH_3CH(OH)CH_3]_3[Al_3P_4O_{16}]$ (APO-IPA) [17], $[N_2C_3H_5]_2[Al_3P_4O_{16}H]$ (APO-ImH) [16], and the surfactant-swollen silicate $[H_2O]_2[NaSrSi_4O_{9.5}]$ (SAMH-3) [15]. We show that these nanocomposite membranes display a substantial reduction of methanol permeability, and that they retain conductivity values in the same order of magnitude as neat Nafion®. We also present small-angle X-ray scattering (SAXS) data showing that the incorporation of these layered materials substantially changes the microstructure of the composite from that of neat Nafion®. We therefore suggest that these inorganic materials offer potentially significant advantages for engineering high-performance fuel cell PEMs.

1.1. Previous approaches for improved PEM performance

There are two main strategies pursued for improvement of PEM performance, focused either on: (i) polymer engineering to synthesize new types of ionomers or (ii) modification of existing PEM ionomers by implementing a methanol barrier. The most comprehensive tests of the performance of a newly developed PEM require a membrane electrode assembly (MEA) [18,19]. Because of the large effort required for reliable MEA fabrication and operation, it is critical to first test the basic performance of the PEM material. Such tests most often include measurements of proton conductivity and methanol permeability, as well as measurements of water and methanol sorption, and thermal/mechanical/chemical stability tests. Often, researchers quantify the conductivity and permeability properties of a DMFC membrane in terms of relative selectivity, which is defined as the ratio of the proton conductivity to the methanol permeability for a given membrane, normalized by the corresponding value for Nafion®.

While polymer engineering efforts are not the focus of the present paper, a number of new synthetic non-fluorinated ionomers are currently investigated [5], such as sulfonated polyimides [20–24], sulfonated polystyrene [25–28], sulfonated polysulfones [29,30], polyether ether ketones [31,32], polyethylenes [33], polyvinyl alcohol [34–37]. Sulfonated/phosphonated polyphosphazene and sulfonated (polyetheretherketone) (SPEEK) were synthesized by sulfonation of a non-fluorinated backbone. These membranes have a low methanol conductivity and good mechanical stability; however, they show significant reduction of proton conductivity. Incorporation of inorganic polymers such as poly-phosphoric-acid into polybenzimidazole (PBI) has also been investigated [35,38]. Such membranes show high proton conductivity and low methanol permeability; but the phosphoric acid groups are not covalently bonded to the polymeric matrix and can leach out of the membrane [11]. Other types of fluorinated membranes have also been commercialized [5,39,40]. The other method for improving PEM performance, which is the subject of this paper, is the modification of Nafion®-based polymer to fabricate composite materials that contain a filler material to act as a methanol barrier. These filler materials include metals (e.g. Pd) [41], clays (e.g. montmorillonite) [42–48], and porous materials such as zeolites [49,50]. Yoon et al. investigated the performance of a PEM made by coating Pd on the surface of Nafion® membranes [41]. These membranes reduced the methanol permeability as well as the proton conductivity. According to Song et al. Nafion®/montmorillonite (MMT) composite membranes (1 wt% of MMT), had 25% lower proton conductivity, and 20 times lower methanol permeability, than Nafion® [51]. Sub-

sequently, Rhee et al. also reported the fabrication of Nafion®/MMT composite membranes [45]. For a 15 wt% of MMT they obtained about an order-of-magnitude reduction in methanol permeability but also a 50% reduction in the conductivity at 303 K. Other investigations (which are all discussed in more detail below) focused on inclusion of MMT in ionomers other than Nafion® [52], the use of other layered clays such as cloisite to form composites with Nafion® [46], and the use of zeolite nanoparticles in Nafion® [49,50,53,54]. An intrinsic limitation of most of the above composite materials is that one cannot independently control the proton transport and the methanol permeation characteristics. Metallic and clay fillers are non-porous, and can only increase the proton conductivity by allowing a high rate of proton hopping on their surfaces. Zeolite nanocrystal fillers have relatively low proton conductivity, although this can be addressed to some extent by the incorporation of sulfonic acid groups [49,53]. They also have a low aspect ratio, which limits the tortuosity of the transport path for methanol.

1.2. Overview of measurement methods

As mentioned earlier, proton conductivity and methanol crossover/permeability measurements are critical for estimating the performance of new PEM materials. However, the literature shows significant variations in the measurement and sample preparation methods, resulting in a range of reported proton conductivity and methanol permeability values. For example, the proton conductivity of Nafion® varies from 0.05 to 0.1 S/cm depending on the measurement procedures and the sample preparation methods [23,35,49,55]. There are two main methods to measure conductivity, viz. the DC-based and AC-based methods. In each case, the electrode configuration can be either a 2-point probe or a 4-point probe. The most consistent measurements were usually done using 4-point probes, after the PEMs were equilibrated in water [35]. The 4-point probe measurements give a conductivity value in the direction parallel to the surface of the membrane (the "in-plane" conductivity). These values are usually higher than those obtained by 2-point probes, which measure the conductivity in the direction perpendicular to the surface of the membrane (the "out-of-plane" conductivity). Furthermore, the PEM can be pre-treated in different ways before conductivity measurements. In some cases, the PEM is simply equilibrated in water, whereas in other cases it is also treated with sulfuric acid and additionally with hydrogen peroxide. The methanol crossover is usually measured with a permeation cell.

1.3. Results of previous works

Fig. 2 collects the results of previous literature on the conductivity and permeability of polymeric and composite PEMs. The results from our work are also shown (points #17 and #18) but will be discussed in the following sections. The technologically desirable region lies to the top left of Fig. 2 (i.e. high conductivity and low methanol permeability). A number of observations can be made from this plot. Firstly, the proton conductivity of pure Nafion® membranes shows only moderate variation depending on the measurement methods and the actual molecular weight of the ionomer used [21–23,35,36,41,44,46,49–51]. However, the methanol permeability shows a significant spread. Several studies report conductivity and permeability data on other polymeric

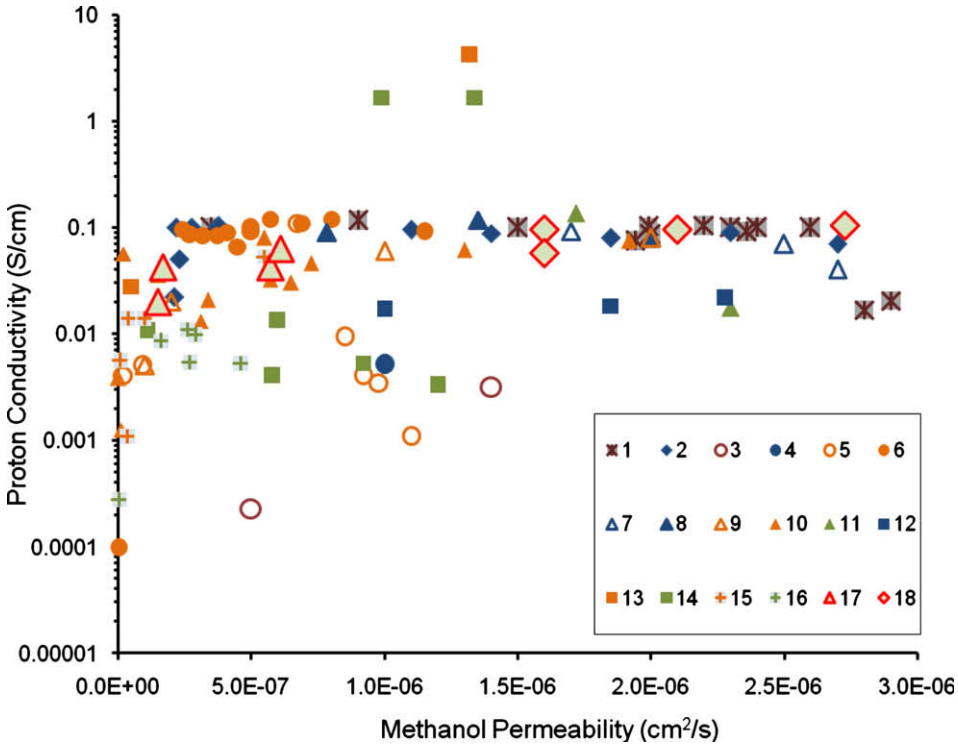

Fig. 2. Proton conductivity (pc) versus methanol permeability (mp) of composite PEMs from the literature as well as the present work: (1) neat Nafion® [21–23,35,36,41,44,46,49–51], (2) Nafion®/nanocomposite, fully activated, 4-point probe [45–49,51], (3) non-fluorinated/nanocomposite, acid activated, 2-point probe [52], (4) Nafion®/nanocomposite, acid activated, 4-point probe [50], (5) non-fluorinated polymer, acid activated, 2-point probe [21,28,31,56], (6) non-fluorinated polymer, acid activated, 4-point probe [20,22–24,27], (7) Nafion®/nanocomposite, water activated, 2-point probe [44], (8) Nafion®/nanocomposite, water activated, 4-point probe [43,57], (9) non-fluorinated polymer, water activated, 2-point probe [19,25,64], (10) non-fluorinated polymer, water activated, 4-point probe [26,32,36,37,59], (11) fluorinated polymer, water activated, 4-point probe [41,58], (12) Nafion®/nanocomposite, salt activated, 4-point probe [50], (13) non-fluorinated polymer, salt activated, 4-point probe [33], (14) fluorinated polymer, salt activated, 4-point probe [33], (15) non-fluorinated polymer, acid activated (pc measurement), water activated (mp measurement), 2-point probe [35], (16) fluorinated polymer, acid activated (pc), water activated (mp), 2-point probe [35], (17) present work, water activated, 4-point probe, and (18) present work, fully activated, 4-point probe. (For interpretation to colours in this figure, the reader is referred to the web version of this paper.)

PEMs after different types of treatments. Of these works, many studies report relatively unfavorable methanol permeabilities greater than 10^{-6} cm^2/s [21–23,35,36,41,44,49–51].

Considering in more detail the works which report favorable methanol permeabilities (below 10^{-6} cm^2/s), the dependence of proton conductivity on the membrane activation method is an important point. Several works report conductivity measurements after equilibrating the PEM in salt solution (points #13 and #14). The proton conductivities of these PEMs are only moderately high. Another work [35] reports conductivity measurements using 2-point probes and after equilibrating the membrane in water prior to measuring the methanol permeability, but equilibrating the membrane in sulfuric acid prior to proton conductivity measurements (points #15 and #16 in Fig. 2). A set of works [19,21,25,28,31,35,44,52,56,64] report conductivity measurements using 2-point probes and after equilibrating the membrane either in water only, or sulfuric acid followed by water, prior to both methanol permeation and proton conductivity measurements (points #3, #5, #7, #9, and #15). The proton conductivities reported in these works are usually rather low, with a couple of exceptions. However, other papers report promising properties using a range of activation treatments. One set of works [45–49,51] employs a full sequence of activation treatment, including treatment in water, sulfuric acid, and hydrogen peroxide (point #2). High proton conductivities and reasonably low methanol permeabilities were obtained. A second set of works [19,25,26,32,36,37,41,43,44,57–59,64] reports measurements only after water treatment (#7–#11). The results are generally promising, although the conductivities are somewhat lower than those obtained from the full activation procedure. Finally, another set of works [20–24,27,28,31,50,52,56] report data after only sulfuric acid treatment, and also achieve promising conductivities and permeabilities (#3–#6). Several works target the inclusion of inorganic fillers into polymeric matrix, and report improvements in proton conductivity and methanol permeability (#2–#4, #7, #8, and #12). Incorporation of intercalated Na-montmorillonite (MMT) in Nafion® has been reported to achieve varying levels of success in reducing methanol permeability and maintaining proton conductivity [44,45]. A work on aluminosilicate cloisite clay/Nafion® composite membranes reports conductivity of the same order of magnitude as Nafion® and a significant reduction of methanol permeability [46]. Acid-functionalized zeolite beta/Nafion® composite membranes also show high proton conductivity and methanol permeability reduction [49]. These works are shown as points # 2 and #8 in Fig. 2.

The preceding discussion highlights the range of previous approaches, measurement conditions, and range of functional properties obtained. Comparison of results obtained by different authors is most useful when the measurement and membrane activation methods used are also similar. The discussion also indicates that there is significant potential for the development of membrane architectures that can allow more independent control over the proton transport and methanol permeability characteristics. The nanocomposite membrane approach has been found to be promising towards this goal. The fabrication of membranes containing inorganic materials of higher functionality than those previously used, is therefore a logical approach and is the motivation for the present paper.

2. Experimental procedures

2.1. Membrane fabrication

Prior to membrane fabrication, the inorganic layered materials were synthesized and purified based on previous reports [14–17]. Subsequently, all the aluminophosphate layered materials were used directly in the polymer matrix during the membrane fabrication. This is because such materials are often easily destroyed by attempts to swell the interlayer spaces with pillaring agents. On the other hand, the AMH-3 layered silicate material was first swollen prior incorporation to the Nafion® solution, due to the better stability of the layer structure during swelling treatments. The detailed procedure for swelling of the AMH-3 layers is reported elsewhere [60]. While AMH-3 is a layered silicate material with 3-D nanoporous layers/slabs of thickness ~1 nm, the aluminophosphate materials are composed of 2-D sheets/nets of even smaller thickness. The structures of these materials are presented in Fig. 3, and their pore dimensions are shown in Table 1. These values correspond to the starting structures and are only indicative of the true pore dimensions, since significant changes of the layer structure may occur during processing [58].

Fabrication of the nanocomposite membranes begins with dispersion of the inorganic layered materials in an organic solvent, followed by the addition of Nafion® solution to make the mixture solution for casting. For example, nanocomposite membranes containing 5 wt% of inorganic layered materials in Nafion® were fabricated by first dispersing 0.05 g of layered material in 0.9 g of isopropanol via ultrasonication. A 20 wt% Nafion® solution in isopropanol and water (Sigma–Aldrich) was concentrated to 26 wt% in a desiccator for 2 weeks prior to use. In a typical membrane synthesis, 4.5 g of the concentrated Nafion® solution was combined with the layered material dispersion, stirred overnight, and then cast on a glass substrate with a 12 mil casting knife (1 mil = 25.4 μm). The cast membrane was kept at room temperature overnight, and then removed from the substrate. It was then annealed at 100 °C for 16 h in a vacuum oven.

2.2. Structural characterization

The microstructure of the membrane samples was characterized by small-angle X-ray scattering (SAXS). This data was obtained at room temperature using a SAXSess instrument (Anton Paar GmbH) operating with Cu Kα radiation.

2.3. Membrane activation

Prior to the measurements (methanol permeability and ionic conductivity), the membranes were activated by chemical treatments. As is well known, the purpose of these treatments is to activate as many sulfonic acid groups as possible, and to remove impurities from the ionomer. However, their effects on polymer/inorganic nanocomposite membranes are not well understood. In this paper we report data from membranes activated by two different sets of techniques employed in the literature: (i) "full activation" (sample code F), and (ii) "water-only activation" (sample code W). In full activation, the annealed membranes were heated in a 5 wt% H_2O_2 solution at 80 °C and any excess H_2O_2 on the sample surface was removed by immersion in deionized (DI) water for 30 min at room temperature. The membranes were then immersed in a 0.5 M H_2SO_4 solution for 2 h at 80 °C, and then rinsed with DI water at room temperature for 30 min. The samples were then stored in DI water for at least 6 h prior to measurements. In "water-only activation", the annealed membranes were kept in DI water for at least 6 h prior to measurements, without further treatments. These two types of samples allow us to quantify the effects of chemical activation treatments on the properties of the membranes in relation to their properties before any such treatments.

2.4. Methanol permeation measurements

Methanol permeation was carried out by sealing the membrane between two cells, each of volume 300 ml. The feed cell initially contained 8 vol% methanol in water, and the permeate cell initially

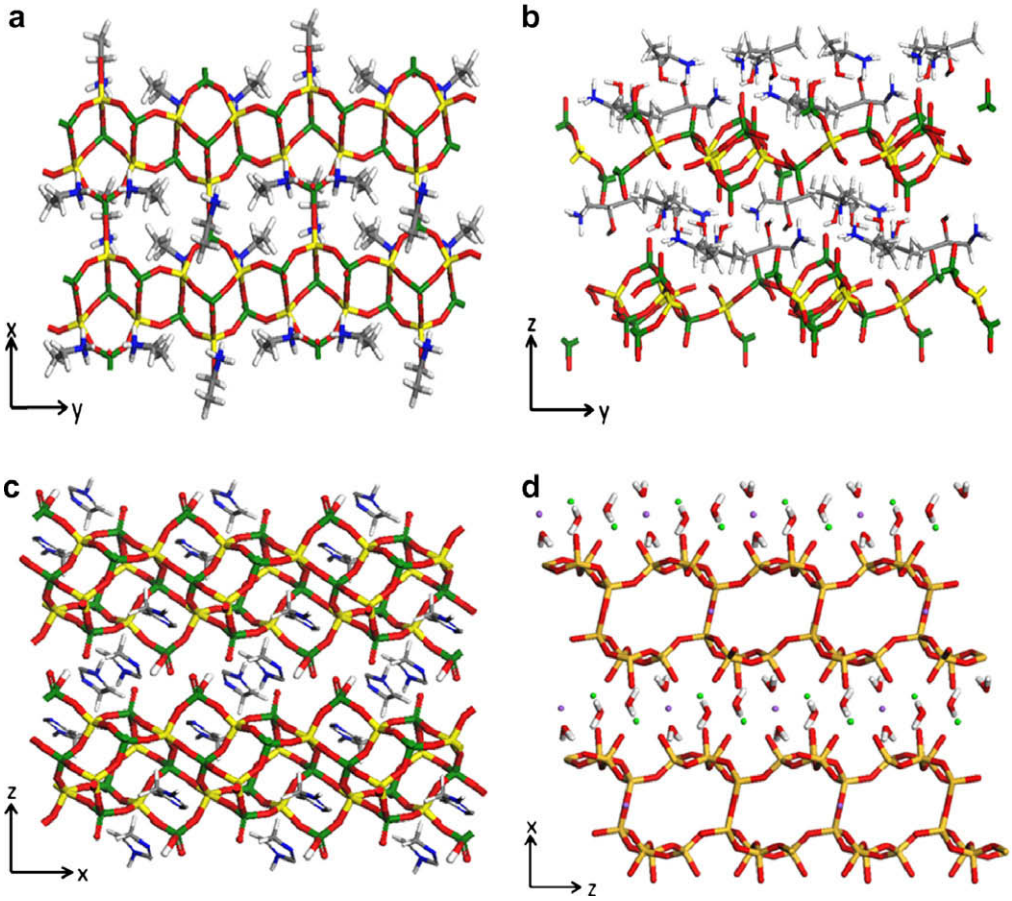

Fig. 3. The crystal structures of the four nanoporous oxide layered materials used in this work: (a) APO-triethylamine (APO-TE), (b) APO-isopropanolamine (APO-IPA), (c) APO-imidazole (APO-ImH), and (d) AMH-3 (gold: silicon, yellow: aluminum, green: phosphorus, red: oxygen, blue: nitrogen, grey: carbon, and white: hydrogen). The swelling agents used to produce SAMH-3 from AMH-3 are not shown. (For interpretation of the references to colour in this figure legend, the reader is referred to the web version of this article.)

Table 1
Crystallographic pore dimensions of layered aluminophosphate and layered silicate materials employed in this work

Material	Pore dimensions (Å)
APO-TE	$4.44 \times 3.29 \times 3.17$
APO-IPA	6.53×6.45
APO-ImH	5.90×2.81
SAMH-3	$4.24 \times 4.10 \times 3.40$

Note that these dimensions do not account for the presence of the organic templates (for the APO materials), nor the metal cations and surfactants (for SAMH-3).

contained pure water. The permeating area was 2.4 cm^2. The methanol concentration in the permeate cell was measured as a function of time using a refractometer. The methanol permeability is then extracted by fitting the data to an unsteady-state permeation model. Two main assumptions were made, both of which are well-justified: (i) the concentration of the methanol in each cell is uniform (ideal mixing) and (ii) the volume in the permeate cell was not affected upon the withdrawal of approximately 100 μL of sample throughout the measurement. For permeation between two cells (1 and 2) of equal volume V, the unsteady-state differential equation is $VC_2'(t) = (AP/L)[C_1(t) - C_2(t)]$, where C_1 and C_2 are the instantaneous methanol concentrations in the two chambers, A is the area of the membrane exposed to the methanol solution, the methanol permeability is P, and the membrane thickness is L. Using the overall mass balance $C_1(t) = [C_1(0) - C_2(t)]$ and integrating the differential equation, we get $C_2(t) = C_1(0)/2[1 - \exp(-2APt/LV)]$. The permeability is obtained by fitting this expression to the experimental data.

2.5. Conductivity measurements

The proton conductivity of the membranes was measured by means of a high-throughput conductivity (HTC) instrument [61], which carries out high-throughput AC impedance spectroscopy in a 4-point probe configuration. The conductivity was measured at a frequency of 1000 Hz and an input amplitude of 10 mV. The conductivity measurements were performed with the membrane being immersed in liquid water at room temperature. Another advantage of the HTC is that many (~20) different sections of the sample (each of area approximately 50 mm^2) can be measured microscopically, thus yielding both average values as well as statistical uncertainties (error bars) with a single (or few) macroscopic sample(s).

3. Results and discussion

3.1. Proton conductivity and methanol permeability

First, we fabricated neat Nafion® membranes with a range of film casting rates used by previous authors, and measured their permeability and conductivity properties to test the influence of this process parameter on the reproducibility of the results. These investigations (results not shown here) make clear that there is no significant influence of the different membrane casting rates on the

methanol permeability and conductivity of Nafion®. As a result, all the nanocomposite samples are justifiably considered to have been prepared in a reproducible manner, and the same process steps (described in Section 2) were applied as exactly as possible to all samples reported here.

Next, we investigated the influence of membrane activation procedures on the properties of Nafion®. We conducted a systematic study in which pure Nafion® membranes were pre-treated sequentially by three different methods: (i) activation only with DI water, (ii) acid activation, in which membranes were pre-treated using only sulfuric acid (H_2SO_4) solution followed by washing in DI water, and (iii) full activation (see Section 2). The membranes were then annealed on an aluminum substrate. Since the thickness of each membrane sample typically displays some variation, this parameter was also measured for each sample using a micrometer. Fig. 4 shows the proton conductivity of the samples as a function of activation conditions. There is a trend of increasing conductivity as the complexity of the activation procedure increases, with the conductivity ranging from ~75 mS/cm for water activated samples to ~90 mS/cm or higher for fully activated samples. The activation procedure was also found to affect the methanol permeability. The water activated sample showed about twice the methanol permeability as the fully activated sample.

We then investigated the proton conductivity and methanol permeability of our nanocomposite membranes. As mentioned in Section 2, the proton conductivity was measured using a high-throughput method [61]. The methanol permeability was measured by fitting a simple permeation model to unsteady-state methanol permeate concentration data. The thickness of each membrane is measured separately after the permeation experiment and is held constant in the model fitting. Fig. 5 illustrates the fit results, which are of high quality. The proton conductivities and methanol permeabilities of the nanocomposite membranes at 25 °C are presented in Table 2. Results from both fully activated membranes (sample code F) and water activated membranes (sample code W) are shown. The average methanol permeability and proton conductivity of the corresponding neat Nafion® membranes are also shown in Table 2. The water activated membranes showed substantial effects of the inorganic material on the permeability and the conductivity. All the water activated nanocomposite membranes had lower conductivities than the neat Nafion® membrane, the reduction in conductivity being at most a factor of 3 and

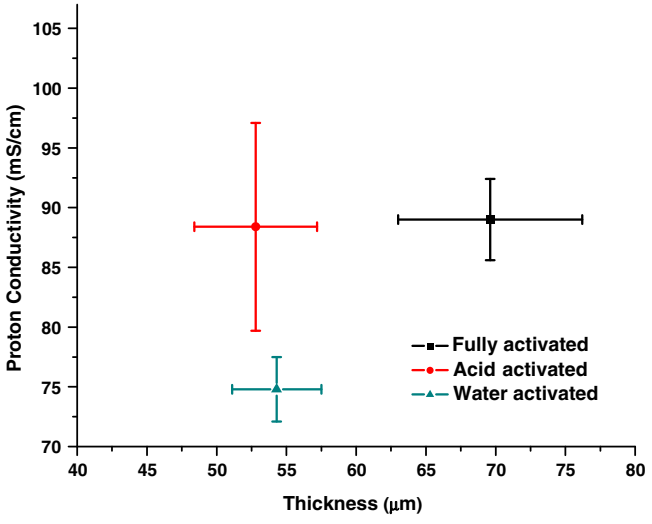

Fig. 4. Dependence of proton conductivity of neat Nafion® membranes on the activation procedures. The membrane thicknesses are also shown on the *x*-axis for reference.

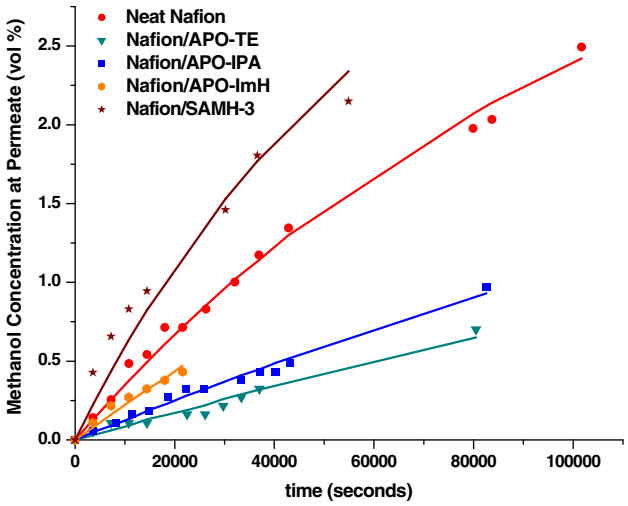

Fig. 5. Representative time-dependent methanol concentration in the permeate cell of inorganic/Nafion® nanocomposite membranes activated by water only. The model fits are shown as solid lines. A few data points were taken at long times to further illustrate the validity of the fitting model.

Table 2
Thickness, proton conductivity, and methanol permeability of nanocomposite and neat Nafion® membranes at two different activation conditions: water activated (W) and fully activated (F)

Membrane	Sample code	Thickness (μm)	Proton conductivity (mS/cm)	Methanol permeability (10^{-6} cm^2/s)
Nafion®	W1	54.3 ± 3.2	74.8 ± 2.7	1.94
Nafion®/SAMH-3	W2	12.7 ± 1.7	42 ± 5	0.57
Nafion®/APO-TE	W3	18.1 ± 3.9	20 ± 4	0.15
Nafion®/APO-ImH	W4	44.5 ± 2.5	63 ± 12	0.61
Nafion®/APO-IPA	W5	29.1 ± 10.4	42 ± 51	0.17
Nafion®	F1	28.1 ± 4.7	117 ± 11.8	0.90
Nafion®/SAMH-3	F2	15.2 ± 2.5	95.7 ± 20.5	2.10
Nafion®/APO-TE	F3	19.3 ± 1.4	95.9 ± 15.4	1.60
Nafion®/APO-ImH	F4	41.7 ± 4.2	104.7 ± 4.2	2.73
Nafion®/APO-IPA	F5	33.6 ± 6.4	57.3 ± 16.5	1.60

The error estimate on the methanol permeability is 6×10^{-8} cm^2/s.

on the average about a factor of 2. However, all the water activated samples uniformly showed a significant reduction in methanol permeability compared to pure Nafion® at least by a factor of 3 and by as much as an order of magnitude. For example, APO-ImH/Nafion®, APO-IPA/Nafion® and SAMH-3/Nafion® nanocomposite membranes showed methanol permeability better than, and proton conductivity comparable to, the neat Nafion® membrane. These results are promising, and clearly show the potential of the proposed approach for independent control of methanol and proton transport through the membrane.

On the other hand, all the membranes showed essentially the same levels of conductivity and permeability as pure Nafion® upon the full activation treatment. The reasons for this behavior are not clear to us at present, and warrant a separate detailed investigation. We hypothesize that the introduction of harsh conditions such as H_2O_2 and acid treatment may have destroyed or disrupted the structure of the layered inorganic materials in the polymer matrix. In the water activated membranes, we do not observe a direct correlation between the pore size of the inorganic material (Table 1) and the performance of the corresponding composite membrane (Table 2). For example, the APO-IPA/Nafion® membrane exhibits the lowest methanol permeability even though its crystallographic pore size is the largest of the inorganic materials. The presence of the polar isopropanolamine molecules in the spaces between the

aluminophosphate layers could also contribute substantially to the control of proton and methanol transport. With respect to layered silicate materials, the SAMH-3/Nafion® nanocomposite membrane shows good performance after swelling of the layers according to our previous work [60]. It is also important to note that a 5 wt% AMH-3/Nafion® composite material, in which the non-swollen AMH-3 crystals remain intact and dispersed in the polymer with no exfoliation or delamination, shows a lower proton conductivity of 32 mS/cm and little reduction in the methanol permeability. The performance of the present membranes is summarized graphically in Fig. 2. The water activated samples are comparable in performance to many of the previous reports that show significant methanol permeability reductions while maintaining similar levels of proton conductivity as pure Nafion®.

3.2. Membrane microstructure

Fig. 6a and b shows SAXS patterns of the W and F nanocomposite membrane samples, along with the corresponding patterns for neat Nafion®. The microstructure of Nafion® has been a subject of considerable debate. A recent overview has been provided by Schmidt-Rohr and Chen [62]. In this study, the SAXS patterns of hydrated neat Nafion® films exhibit the expected features. As the magnitude (Q) of the scattering vector decreases, a sharp increase in scattering intensity at $Q \sim 1\ nm^{-1}$ is observed as a shoulder or as a distinct peak. This "ionomer feature" is attributed to Bragg-like scattering from the water channels (which have been proposed to be cylindrical, spherical, bundle-like, or layered structures). This feature progressively disappears as the membrane is hydrated [63]. The fully hydrated membranes shown in Fig. 6 do not exhibit a prominent ionomer peak, whereas membranes prepared by progressive drying exhibited the ionomer peak. The much slower increase in intensity below $Q \sim 1\ nm^{-1}$ is characteristic of the semicrystalline hydrophobic domains in the material. The upturn in scattering intensity at low-Q ($\sim$0.2 nm^{-1}) is due to the longer-range structural correlations between the water clusters/channels. Steeper upturns are proposed to indicate better-aligned water clusters/channels [62]. In this study, the only significant difference between W and F samples of neat Nafion® appears to be a somewhat larger number/size of crystalline domains after full activation. In the case of the water activated (W) samples, the formation of composite membranes with the layered aluminophosphate (APO) and SAMH-3 materials does not appear to have a significant impact on the high-Q region of the SAXS patterns. The lack of Bragg diffraction peaks from the inorganic materials (at a significant loading of 5 wt%) indicates that a high degree of exfoliation of the inorganic layers has occurred. The low-Q region is significantly altered and the upturn at low angles is much weaker than in the neat Nafion® film. This may be due to a combination of several factors, including the disruption of structural alignment between the water clusters due to the inorganic material, as well as the different Q-dependence of the scattering intensity from the high-aspect-ratio layers. The F samples, which are fully activated, overall exhibit different microstructures from the W samples. Depending upon the layered material, the structure of these membranes differs to varying extents from that of the corresponding neat Nafion®. At present, the reasons for these structural changes, and their correlation with the observed permeability and conductivity, are not well understood. The main result of the present SAXS measurements is that both the formation of the composite membranes, as well as the activation procedures on those composite membranes, yield microstructures that appear quite different from those of the corresponding neat Nafion® membranes. A better understanding of these microstructural effects will be needed in order to form reliable correlations with the functional properties.

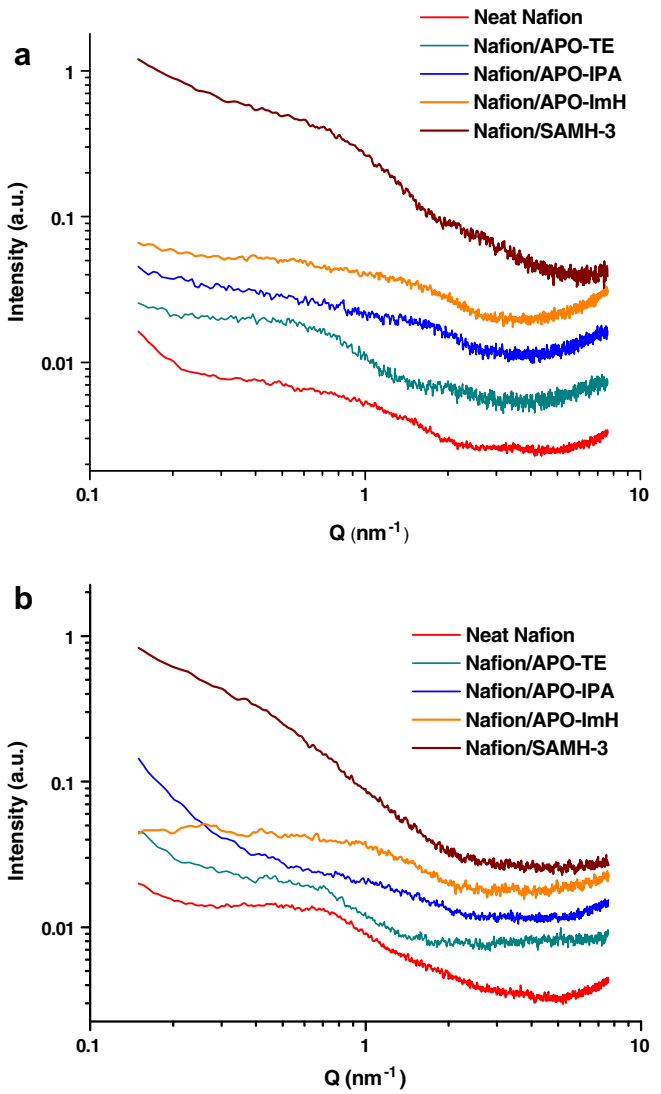

Fig. 6. Small-angle X-ray scattering (SAXS) patterns of neat Nafion®, Nafion®/APO-ethylamine, Nafion®/APO-isopropanolamine, Nafion®/APO-imidazole, and Nafion®/SAMH-3 membranes: (a) before activation (W samples) and (b) after full activation (F samples). The spectra are stacked for clarity.

4. Conclusion

In this paper, we introduced the novel concept of using porous layered inorganic oxide materials to control the proton conductivity and methanol permeability of ionomer membranes for DMFC applications. We prepared nanocomposite membranes containing 5 wt% of such materials exfoliated, intercalated and dispersed in Nafion®. We found that this first set of composite membranes can offer substantial reductions in methanol permeability while maintaining proton conductivity, and moreover have substantially different microstructure in relation to neat Nafion®. We placed our results in context of the state-of-the-art in the development of improved PEM materials for DMFCs, and showed that the proposed approach is comparable to the most promising results available in the literature. We also highlighted the importance of accounting for variations in some of the key experimental methods while comparing results of different researchers.

Acknowledgments

We acknowledge funding for this work from NSF (CHE-9876674, CBET-0327811, CBET-0403574, and CBET-0437621). We

also acknowledge J. Sheffel (U. Minnesota) and C. Gallagher (Georgia Tech) for assistance with sample preparation, and P. Zapata and Prof. J.C. Meredith (Georgia Tech) for assistance with high-throughput proton conductivity data collection.

References

[1] L. Carrette, K.A. Friedrich, U. Stimming, Chem. Phys. Chem. 1 (2000) 162–193.
[2] L. Schlapbach, A. Zuttel, Nature 414 (2001) 353–358.
[3] R.F. Service, Science 296 (2002) 1222–1224.
[4] R. Dillon, S. Srinivasan, A.S. Aricom, V. Antonucci, J. Power Sources 127 (2004) 112–126.
[5] V. Neburchilov, J. Martin, H.J. Wang, J.J. Zhang, J. Power Sources 169 (2007) 221–238.
[6] M. Inaba, T. Kinumoto, M. Kiriake, R. Umebayashi, A. Tasaka, Z. Ogumi, Electrochim. Acta 51 (2006) 5746–5753.
[7] T. Kinumoto, M. Inaba, Y. Nakayama, K. Ogata, R. Umebayashi, A. Tasaka, Y. Iriyama, T. Abe, Z. Ogumi, J. Power Sources 158 (2006) 1222–1228.
[8] A.K. Sahu, G. Selvarani, S. Pitchumani, P. Sridhar, A.K. Shukla, N. Narayanan, A. Banerjee, N. Chandrakumar, J. Electrochem. Soc. 155 (2008) B686–B695.
[9] K. Teranishi, K. Kawata, S. Tsushima, S. Hirai, Electrochem. Solid State Lett. 9 (2006) A475–A477.
[10] W.J. Stevens, Workshop on Basic Research for Hydrogen Production, Storage and Use, 2003. <www1.eere.energy.gov/hydrogenandfuelcells/pdfs/stevens_sc_overview.pdf>.
[11] A.S. Arico, S. Srinivasan, V. Antonucci, Fuel Cells 1 (2001) 133–161.
[12] N.W. Deluca, Y.A. Elabd, J. Polym. Sci., Part B: Polym. Phys. 44 (2006) 2201–2225.
[13] J. Jagur-Grodzinski, Polym. Adv. Technol. 18 (2007) 785–799.
[14] Q.M. Gao, B.Z. Li, J.S. Chen, S.G. Li, R.R. Xu, I. Williams, J.Q. Zheng, D. Barber, J. Solid State Chem. 129 (1997) 37–44.
[15] H.K. Jeong, S. Nair, T. Vogt, L.C. Dickinson, M. Tsapatsis, Nat. Mater. 2 (2003) 53–58.
[16] J.H. Yu, I.D. Williams, J. Solid State Chem. 136 (1998) 141–144.
[17] H.M. Yuan, G.S. Zhu, J.S. Chen, W. Chen, G.D. Yang, R.R. Xu, J. Solid State Chem. 151 (2000) 145–149.
[18] Z.G. Shao, X. Wang, I.M. Hsing, J. Membr. Sci. 210 (2002) 147–153.
[19] R. Wycisk, J.K. Lee, P.N. Pintauro, J. Electrochem. Soc. 152 (2005) A892–A898.
[20] B.R. Einsla, Y.S. Kim, M.A. Hickner, Y.T. Hong, M.L. Hill, B.S. Pivovar, J.E. McGrath, J. Membr. Sci. 255 (2005) 141–148.
[21] C.H. Lee, Y.Z. Wang, J. Polym. Sci., Part A: Polym. Chem. 46 (2008) 2262–2276.
[22] K. Okamoto, Y. Yin, O. Yamada, M.N. Islam, T. Honda, T. Mishima, Y. Suto, K. Tanaka, H. Kita, J. Membr. Sci. 258 (2005) 115–122.
[23] Y. Yin, J.H. Fang, Y.F. Cui, K. Tanaka, H. Kita, K. Okamoto, Polymer 44 (2003) 4509–4518.
[24] F.X. Zhai, X.X. Guo, J.H. Fang, H.J. Xu, J. Membr. Sci. 296 (2007) 102–109.
[25] Y.A. Elabd, C.W. Walker, F.L. Beyer, J. Membr. Sci. 231 (2004) 181–188.
[26] P. Piboonsatsanasakul, J. Wootthikanokkhan, S. Thanawan, J. Appl. Polym. Sci. 107 (2008) 1325–1336.
[27] S. Roualdes, I. Topala, H. Mahdjoub, V. Rouessac, P. Sistat, J. Durand, J. Power Sources 158 (2006) 1270–1281.
[28] J.P. Shin, B.J. Chang, J.H. Kim, S.B. Lee, D.H. Suh, J. Membr. Sci. 251 (2005) 247–254.
[29] F. Lufrano, V. Baglio, P. Staiti, A.S. Arico, V. Antonucci, Desalination 199 (2006) 283–285.
[30] F. Lufrano, V. Baglio, P. Staiti, A.S. Arico, V. Antonucci, J. Power Sources 179 (2008) 34–41.
[31] L. Li, J. Zhang, Y.X. Wang, J. Membr. Sci. 226 (2003) 159–167.
[32] B.P. Tripathi, V.K. Shahi, J. Colloid Interf. Sci. 316 (2007) 612–621.
[33] K. Scott, W.M. Taama, P. Argyropoulos, J. Membr. Sci. 171 (2000) 119–130.
[34] D.S. Kim, H.B. Park, J.W. Rhim, Y.M. Lee, J. Membr. Sci. 240 (2004) 37–48.
[35] B.S. Pivovar, Y.X. Wang, E.L. Cussler, J. Membr. Sci. 154 (1999) 155–162.
[36] J.L. Qiao, T. Hamaya, T. Okada, Polymer 46 (2005) 10809–10816.
[37] J.W. Rhim, H.B. Park, C.S. Lee, J.H. Jun, D.S. Kim, Y.M. Lee, J. Membr. Sci. 238 (2004) 143–151.
[38] J.S. Wainright, J.T. Wang, D. Weng, R.F. Savinell, M. Litt, J. Electrochem. Soc. 142 (1995) L121–L123.
[39] A. Kuver, K. Potje-Kamloth, Electrochim. Acta 43 (1998) 2527–2535.
[40] M. Yoshitake, Y. Kunisa, E. Endoh, E. Yanagisawa, US Patent 6,933,071, 2005.
[41] S.R. Yoon, G.H. Hwang, W.I. Cho, I.H. Oh, S.A. Hong, H.Y. Ha, J. Power Sources 106 (2002) 215–223.
[42] D.H. Jung, S.Y. Cho, D.H. Peck, D.R. Shin, J.S. Kim, J. Power Sources 118 (2003) 205–211.
[43] Y.F. Lin, C.Y. Yen, C.H. Hung, Y.H. Hsiao, C.C.M. Ma, J. Power Sources 168 (2007) 162–166.
[44] Y.F. Lin, C.Y. Yen, C.C.M. Ma, S.H. Liao, C.H. Hung, Y.H. Hsiao, J. Power Sources 165 (2007) 692–700.
[45] C.H. Rhee, H.K. Kim, H. Chang, J.S. Lee, Chem. Mater. 17 (2005) 1691–1697.
[46] J.M. Thomassin, C. Pagnoulle, D. Bizzari, G. Caldarella, A. Germain, R. Jerome, E-Polymer (2004) 18.
[47] J.M. Thomassin, C. Pagnoulle, D. Bizzari, G. Caldarella, A. Germain, R. Jerome, Solid State Ion. 177 (2006) 1137–1144.
[48] J.M. Thomassin, C. Pagnoulle, G. Caldarella, A. Germain, R. Jerome, Polymer 46 (2005) 11389–11395.
[49] Z.W. Chen, B. Holmberg, W.Z. Li, X. Wang, W.Q. Deng, R. Munoz, Y.S. Yan, Chem. Mater. 18 (2006) 5669–5675.
[50] V. Tricoli, F. Nannetti, Electrochim. Acta 48 (2003) 2625–2633.
[51] M.-K. Song, S.-B. Park, Y.-T. Kim, H.-W. Rhee, Mol. Cryst. Liq. Cryst. Sci. Technol., Sect. A 407 (2003) 15–23.
[52] J.H. Chang, J.H. Park, G.G. Park, C.S. Kim, O.O. Park, J. Power Sources 124 (2003) 18–25.
[53] B.A. Holmberg, S.J. Hwang, M.E. Davis, Y.S. Yan, Micropor. Mesopor. Mater. 80 (2005) 347–356.
[54] J.C. McKeen, Y.S. Yan, M.E. Davis, Chem. Mater. 20 (2008) 3791–3793.
[55] S. Slade, S.A. Campbell, T.R. Ralph, F.C. Walsh, J. Electrochem. Soc. 149 (2002) A1556–A1564.
[56] R. Thangamuthu, C.W. Lin, Solid State Ion. 176 (2005) 531–538.
[57] W.L. Xu, T.H. Lu, C.P. Liu, W. Xing, Electrochim. Acta 50 (2005) 3280–3285.
[58] M. Shen, S. Roy, J.W. Kuhlmann, K. Scott, K. Lovell, J.A. Horsfall, J. Membr. Sci. 251 (2005) 121–130.
[59] X.Y. Zhou, J. Weston, E. Chalkova, M.A. Hofmann, C.M. Ambler, H.R. Allcock, S.N. Lvov, Electrochim. Acta 48 (2003) 2173–2180.
[60] S. Choi, J. Coronas, E. Jordan, W. Oh, S. Nair, F. Onorato, D.F. Shantz, M. Tsapatsis, Angew. Chem., Int. Ed. 47 (2008) 552–555.
[61] J.C. Meredith, J. Mater. Sci. 38 (2003) 4427–4437.
[62] K. Schmidt-Rohr, Q. Chen, Nat. Mater. 7 (2008) 75–83.
[63] G. Gebel, O. Diat, Fuel Cells 5 (2005) 261–276.
[64] Y.G. Jin, J.C.D. da Costa, G.Q. Lu, Solid State Ion. 178 (2007) 937–942.